Sensors and Actuators A 313 (2020) 112210

Contents lists available at ScienceDirect

Sensors and Actuators A: Physical

journal homepage: www.elsevier.com/locate/sna

Short communication

Perfect collocation using self-sensing electromagnetic actuator: Application to vibration control of flexible structures

Mohit Verma [a,*], Vicente Lafarga [b], Christophe Collette [b,c]

[a] CSIR - Structural Engineering Research Centre, CSIR Campus, Taramani, Chennai - 600 113, India
[b] Université Libre de Bruxelles, Precision Mechatronics Laboratory, BEAMS Department, 50, F.D. Roosevelt Av., 1050 Brussels, Belgium
[c] University of Liège, Department of Aerospace and Mechanical Engineering, Allée de la Découverte 9, 4000 Liège, Belgium

ARTICLE INFO

Article history:
Received 11 May 2020
Received in revised form 6 July 2020
Accepted 15 July 2020
Available online 17 July 2020

Keywords:
Vibration isolation
Self-sensing
Collocated control
Active damping
Electromagnetic actuator

ABSTRACT

Collocated control has the advantages of robustness and guaranteed stability. In collocated control, the sensor and actuator are placed close to each other. True collocation can be achieved using self-sensing in which the actuator can also be used as a sensor. In this article, we present a self-sensing electromagnetic actuator for vibration control of flexible structures. The back electromotive force (emf) generated in the coil is measured to evaluate the velocity of the structure (and hence, the displacement). The position measurements obtained from self-sensing are found to have good correlation with those obtained using an eddy current sensor. The efficacy of the proposed technique has been verified for the vibration control of a flexible cantilever beam. Self-sensing offers economical, simple and robust control architecture. It can be effectively used for applications where sensors and actuators cannot be collocated due to space and size limitations.

1. Introduction

External disturbances like ground motion or environmental disturbances can greatly affect the performance of the sensitive equipment. Active systems can be used to isolate the equipment from the external disturbances [1]. Sensors and actuators in many active systems are often collocated in order to build robustness into the system. The open loop transfer function of collocated systems has alternating poles and zeros on the imaginary axis. In such systems, the stability is guaranteed as the phase lag due to each pole is compensated by the phase lead due to the corresponding zero [2]. The collocation of sensors and actuators is however not possible at all times. There might be space restrictions in certain applications. One might encounter a situation where the size of the sensor is not negligible in comparison to the main structure. In such cases, the mechanical impedance of the structure is greatly modified when the sensors are installed on the structure.

Self-sensing provides an alternative to overcome these problems. Perfect collocation can be achieved using self-sensing in which a single transducer is used as an actuator and sensor concurrently. It offers a simple, robust and cost-effective solution for collocated control. Self-sensing reduces the complexity by reducing the number of actuators and sensors in the system. It also leads to reduction in the power requirements and the wiring used in the instrumentation. Sensors are more prone to failure compared to the actuators in the control system [3]. Thus, self-sensing also leads to a robust system as a single transducer serves the dual purpose of sensing and actuation. Many self-sensing transducers have been developed in the past using different types of active materials. Self-sensing using piezoelectric materials have been used for measuring stress, force and position [4–7]. A dielectric elastomer actuator has been used for position sensing and force control [8,9]. In some recent applications, shape memory alloys [10] and magnetorheological fluid [11] based actuators have also been used for self-sensing. Electromagnetic actuators have been used for velocity, position and force estimations [12–14].

In this article, we present a self-sensing electromagnetic actuator for vibration control of flexible structures. The present scheme does not require any modifications to the design of the electromagnetic actuator. It takes advantage of the fact that the voltage drop across the coil can be measured and related to its motion. The electromagnetic actuator is operated in current mode. It does not require an additional bridge structure for measuring the voltage drop across the coil (which is usually required if the actuator is operated in voltage mode). The organization of this article is as follows: Section 2 presents comparison of collocated control with the

* Corresponding author.
E-mail address: mohitverma@serc.res.in (M. Verma).

https://doi.org/10.1016/j.sna.2020.112210
0924-4247/

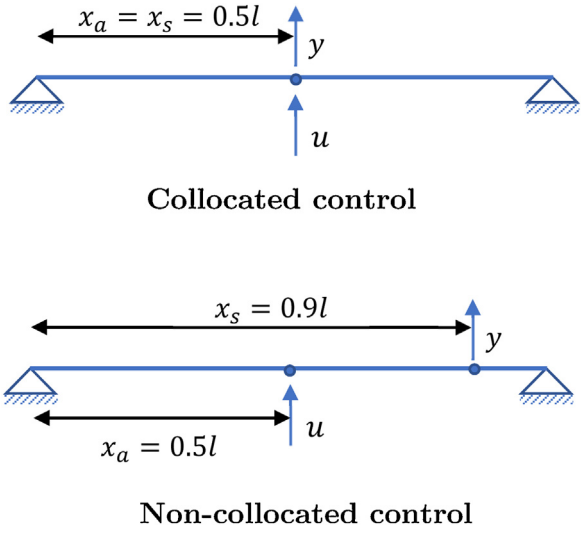

Fig. 1. Location of actuator and sensor for collocated and non-collocated control.

non-collocated control. The concept of self-sensing using electromagnetic actuator is presented in Section 3. The proof-of-concept experiments carried out to validate self-sensing are explained in Section 4. The envisioned application for self-sensing is presented in Section 5, which is followed by concluding remarks in Section 6.

2. Collocated vs non-collocated control

In order to highlight the advantages of the collocated control over non-collocated control, we consider a case of a continuous beam pinned at both the ends. Using Euler–Bernoulli beam theory, the dynamics of the beam can be written as the following partial differential equation

$$\frac{\partial^2}{\partial x^2}\left(EI\frac{\partial^2 w}{\partial x^2}\right) + m\frac{\partial^2 w}{\partial t^2} = p \tag{1}$$

where w is the displacement, EI represents the bending stiffness, m is the mass per unit length and p is the external load per unit length. For a case of free vibration and harmonic solution of the form $w(x, t) = \phi(x)e^{j\omega t}$, the above partial differential equation is reduced to the following ordinary differential equation

$$\frac{d^4\phi}{dx^4} - \frac{m}{EI}\omega^2\phi = 0 \tag{2}$$

The above equation is an eigenvalue problem whose solutions are ω_i and ϕ_i representing natural frequencies and corresponding mode shapes, respectively. For a beam pinned at both the ends, the natural frequencies and the mode shapes are

$$\begin{aligned} \omega_i^2 &= (i\pi)^4 \frac{EI}{ml^4} \\ \phi_i(x) &= \sin\frac{i\pi x}{l} \end{aligned} \tag{3}$$

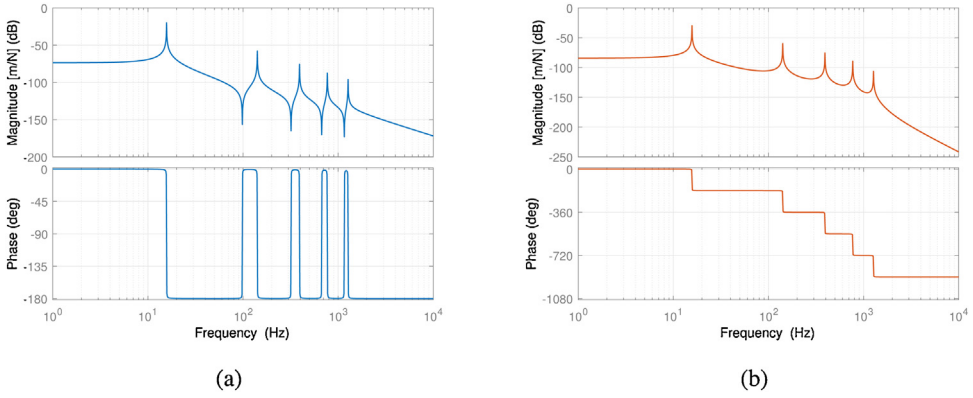

Fig. 2. Frequency responses of the open loop transfer function from actuator force to the displacement measured by the sensor in case of – (a) collocated control and (b) non-collocated control.

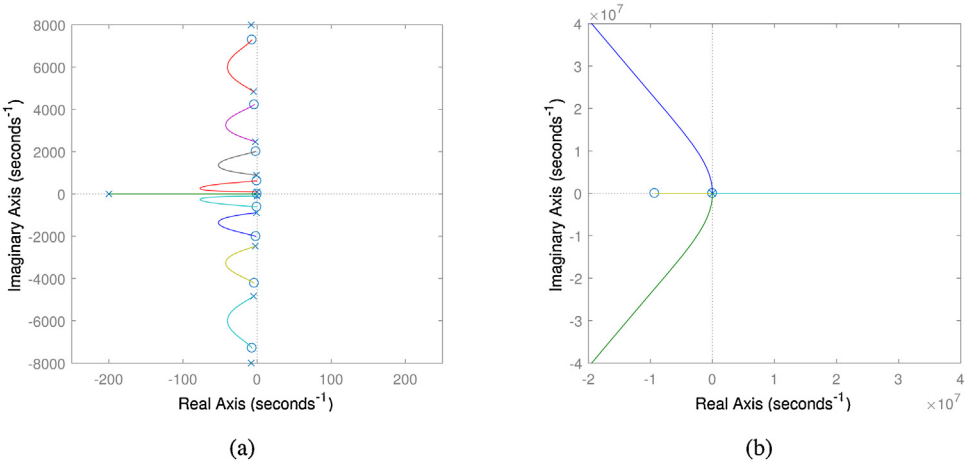

Fig. 3. Root locus with lead compensator for – (a) collocated control and (b) non-collocated control.

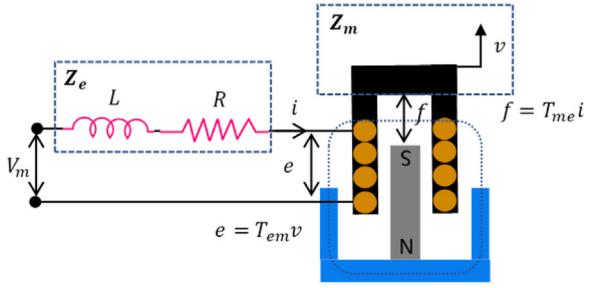

Fig. 4. Model of electromagnetic actuator.

where l is the length of the beam. The frequency response between the actuator force, u, at point x_a and sensor displacement, y, at point x_b can be written as [15]

$$G(s) = \frac{y}{u} = \sum_{i=1}^{\infty} \frac{\phi_i(x_a)\phi_i(x_b)}{\mu_i(s^2 + 2\xi_i\omega_i s + \omega_i^2)} \tag{4}$$

where μ_i is the generalized mass (equal to $ml/2$ for a beam pinned at both the ends) and ξ_i is the damping associated with the ith mode. The series expansion can be limited to a finite number of modes in case of a discrete system. The sensor and actuator location for collocated and non-collocated control are shown in Fig. 1. In case of collocated control it is assumed that both the actuator and sensor are located at $x_a = x_s = 0.5l$. For non-collocated control, it is assumed that the actuator is located at mid span ($x_1 = 0.5l$) while the sensor is placed at $x_s = 0.9l$. The bending stiffness, EI, of the beam is taken as 100 N m^2, mass per unit length, m, is taken as 1 kg/m and length, l, is taken as 1 m. The first ten modes are considered for evaluation of the open loop transfer function. The open loop transfer functions from actuator force to the sensor displacement for collocated and non-collocated controls are shown in Fig. 2a and b, respectively. It is observed that the collocated system has alternating poles and zeros. The phase drop due to each pole is compensated by the phase gain due to zero. The phase of the open loop transfer function is bounded between 0 and π. This interlacing property of the collocated system provides asymptotic stability even when the system parameters are subjected to large variations. Collocated system provides robust stability to the system. However, this pole-zero interlacing property does not exist in the non-collocated system. The phase is not bounded between 0 and π and the system is not robustly stable. This fact is further illustrated by studying the root locus of the feedback system. The system is assumed to have a following lead compensator in the feedback loop

$$K(s) = \frac{10s + 1}{0.005s + 1} \tag{5}$$

The root loci of the collocated and non-collocated systems are shown in Fig. 3a and b, respectively. It can be seen that for collocated system the root locus lies entirely in the left half plane. This means that the system is stable for any value of the gain. The root locus of the non-collocated system does not lie entirely in the left half plane. This implies that for certain values of the gain the closed loop poles of the system will move to the right half plane resulting in an unstable system. Due to the pole-zero interlacing property and robustly stable nature, collocated systems are usually preferred wherever possible.

Table 1
Goodness of fit between the displacement signals obtained from eddy current sensor and self-sensing.

Root mean squared error (RMSE)	Sum of squared error (SSE)	Coefficient of determination (R^2)
0.0072	1.939	0.9927

3. Self-sensing electromagnetic actuator

The model of the electromagnetic actuator is shown in Fig. 4. The actuator can be driven by either a voltage or current source. The

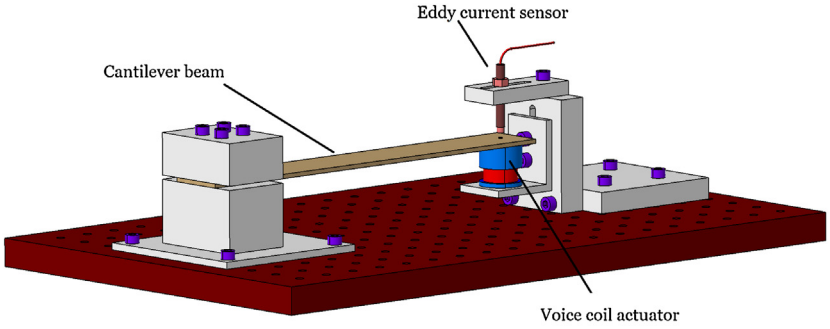

(a)

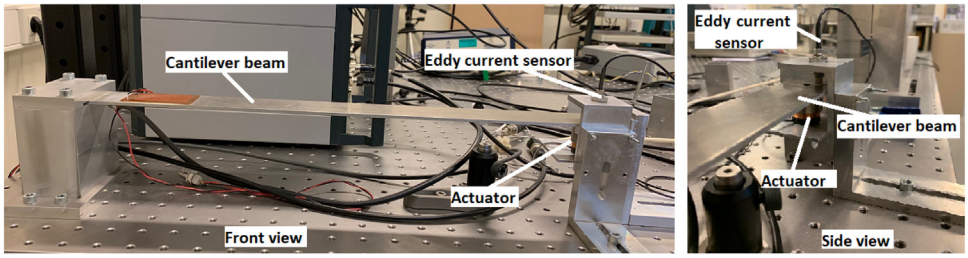

(b)

Fig. 5. Test setup used for proof of concept experiment — (a) schematics and (b) actual setup.

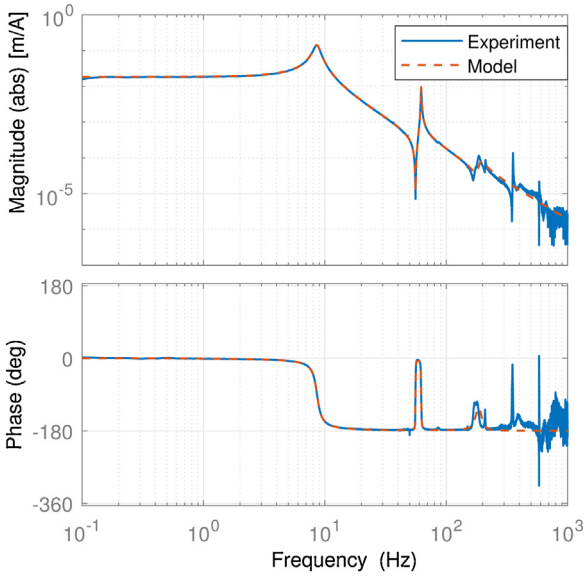

Fig. 6. Comparison of the frequency responses obtained from the experiment and the model. A good match between the experiments and the model is observed up to 100 Hz.

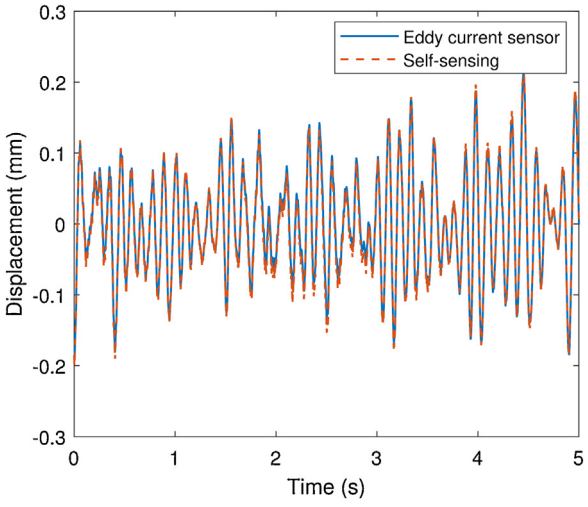

Fig. 7. Comparison of the displacement response of the free end of cantilever beam obtained from self-sensing with that obtained from eddy current sensor.

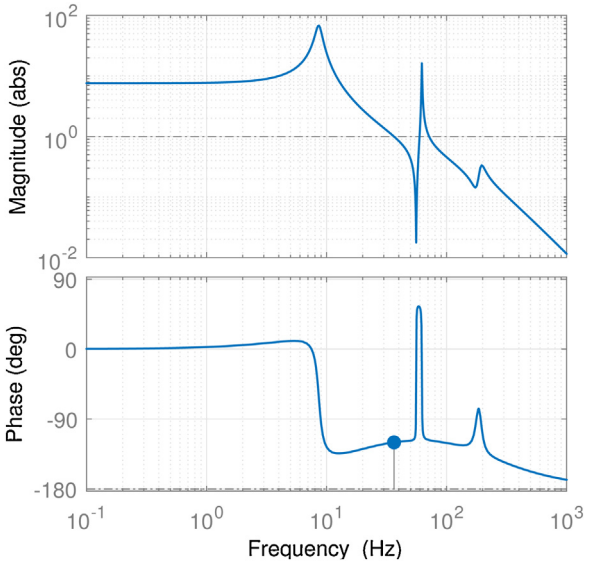

Fig. 8. Open loop gain of the plant with the designed lead controller. The designed controller has a crossover frequency at 36.5 Hz and has a phase margin of 60°.

modeling of the actuator depends on the mode in which it is operated. The constitutive equations of the electromagnetic transducer can be written as

$$\begin{aligned} V_m &= Z_e i + T_{em} v \\ F &= T_{me} i + Z_m v \end{aligned} \tag{6}$$

where V_m is the voltage drop across the terminals of the actuator coil, Z_e is the electrical impedance of the coil, i is the current flowing in the coil, T_{em} is a coupling coefficient representing the back emf constant of the coil, v is the velocity of the mechanical structure, F is the force acting on the mechanical structure attached to the actuator, T_{me} is the coupling coefficient representing the force to current ratio of the actuator and Z_m is the mechanical impedance of the attached structure. The operation of the electromagnetic actuator with a current source ensures that the desired current flows in the coil irrespective of the back emf generated by the motion of the mechanical structure. The losses due to back emf are compensated by the amplifier. Using Kirchoff's law, the voltage drop across the terminals of the coil can be written as

$$V_m = Ri + L\frac{di}{dt} + T_{em} v \tag{7}$$

where R and L are the resistance and inductance of the coil, respectively. Given the parameters R, L and T_{em} of the actuator, the above

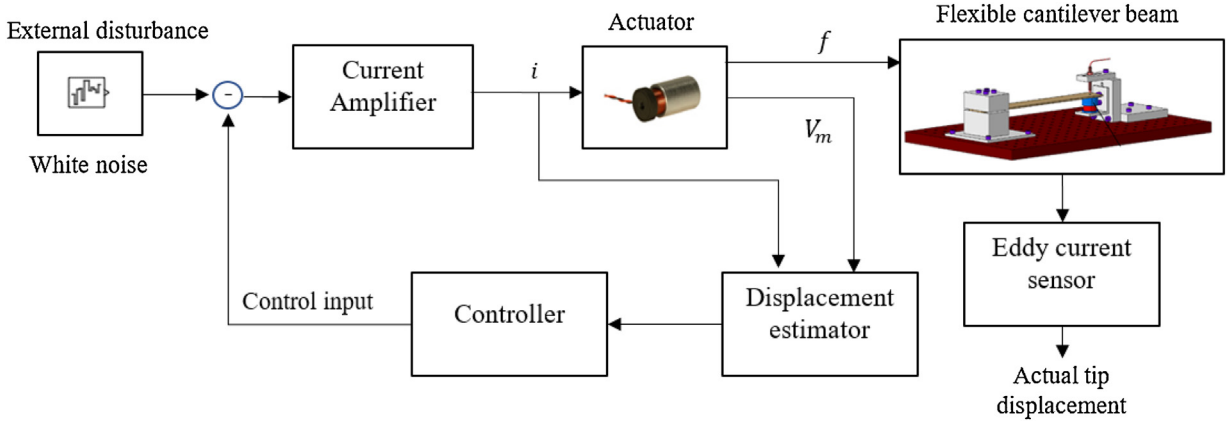

Fig. 9. Block diagram for the experimental verification of self-sensing.

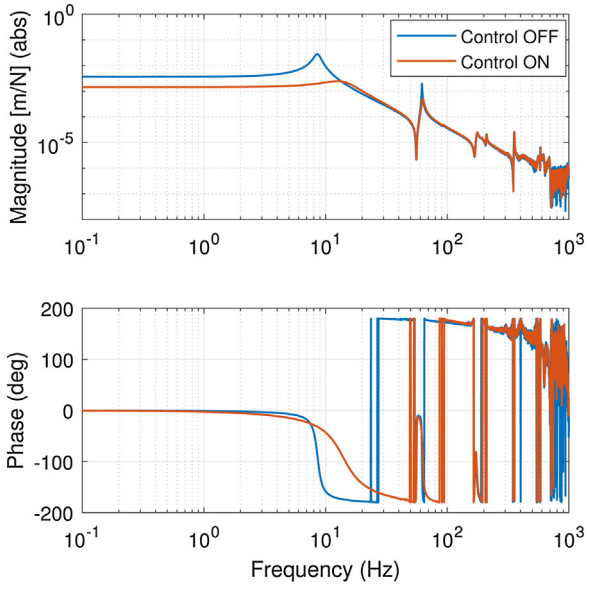

(a)

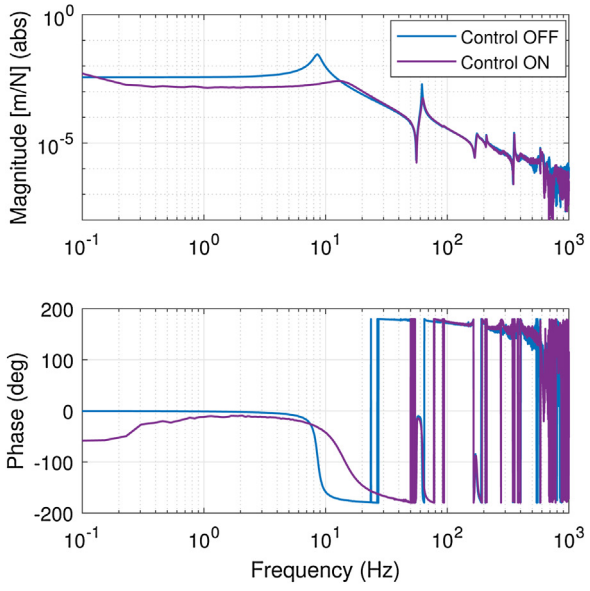

(b)

Fig. 10. Comparison of the frequency responses of the controlled and uncontrolled structure using feedback from — (a) eddy current sensor and (b) self-sensing.

equation shows that it is possible to evaluate the velocity of the mechanical structure by measuring the voltage drop across the terminals of the coil. The velocity of the mechanical structure is related to V_m and i by the following equation

$$v = \frac{V_m - Ri - L\frac{di}{dt}}{T_{em}} \tag{8}$$

Taking the Laplace transform of the above equation, we get

$$v = \frac{V_m - (R + Ls)i}{T_{em}} \tag{9}$$

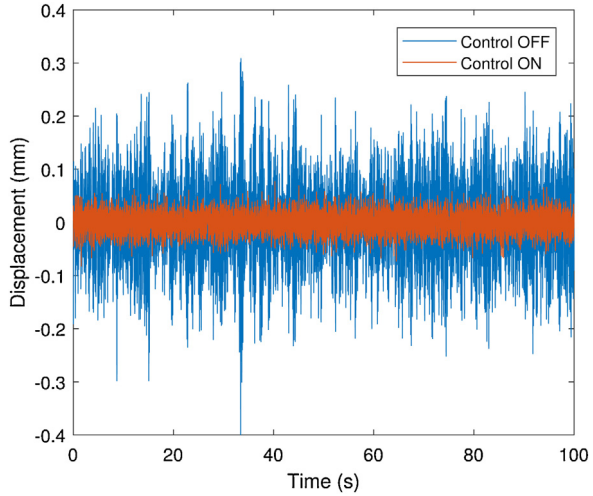

Fig. 11. Comparison of the time domain displacement response of the beam with and without control obtained using self-sensing.

where s is the Laplace transform variable. The displacement of the mechanical structure is given by

$$x = \frac{1}{sT_{em}}V_m - \frac{(R + Ls)}{sT_{em}}i \tag{10}$$

In-house manufactured current amplifier is used in order to operate the electromagnetic actuator in current mode. The circuit diagram of the current amplifier is shown in Fig. A.13 of Appendix A.

4. Proof of concept experiment

The validation of the self-sensing electromagnetic actuator is carried out on a cantilever beam clamped at one end and attached to the voice coil actuator on the other end. The test setup used is shown in Fig. 5. An eddy current sensor is used to track the motion of the free end of cantilever beam. Self-sensing in current mode is used for the proof of concept experiment due to its simplicity, ease of implementation, and availability of the current source.

4.1. Identification of the plant

The plant is identified experimentally by evaluating the frequency response from the input current to the displacement of the free end of the cantilever beam. A white noise signal is injected in the actuator and the displacement is recorded using the eddy current sensor. A transfer function of the plant ($G(s)$) is then obtained using `fitfrd` function in MATLAB [16]. The order of the transfer function is chosen such that it is able to capture all the modes of the plant up to 200 Hz. The transfer function of the plant is

$$G(s) = \frac{76.386(s^2 + 25.82s + 1494)(s^2 + 1.803s + 1.23e05)(s^2 + 144.2s + 1.268e06)}{(s^2 + 25.87s + 1491)(s^2 + 6.88s + 2932)(s^2 + 3.461s + 1.528e05)(s^2 + 144s + 1.451e06)} \tag{11}$$

The frequency responses obtained from the experiment and the model are compared in Fig. 6. The first bending mode of the beam is at 8.6 Hz. It is observed that the frequency response obtained from the experiments matches well with that obtained from the model up to 200 Hz.

4.2. Displacement from self-sensing

The displacement of the free end of the beam is evaluated using Eq. (10). The parameters of the electromagnetic actuator R, L and T_{em} are found to be 6.2 Ω, 1.23 mH and 3.9 Vs/m, respectively. The

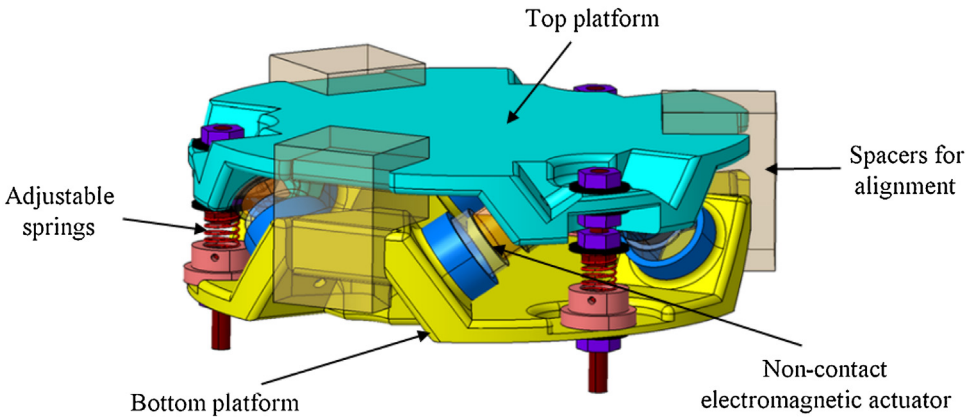

Fig. 12. Configuration of the proposed isolation system for drone camera stabilization.

displacement obtained using Eq. (10) is passed through a high-pass filter in order to avoid the drift due to integration. The cutoff frequency of the filter is set to 0.2 Hz. The displacement response obtained from self-sensing is compared with that obtained from an eddy current sensor in Fig. 7. The displacement response obtained from self-sensing and the eddy current sensor are found to match well with each other. The goodness of fit, defined in terms of root mean squared error (RMSE), sum of squared error (SSE) and coefficient of determination (R^2), between the displacement responses of the beam obtained from the eddy current sensor and self-sensing are given in Table 1.

4.3. Active vibration control

A displacement feedback controller is designed to control the vibrations of the free end of cantilever beam. A lead controller is designed to have sufficient gain margin near the crossover frequency. The designed controller has a crossover frequency at 36.5 Hz and has a phase margin of 60°. The transfer function of the designed controller, $H(s)$, is

$$H(s) = \frac{6094(s + 95.54)}{(s + 1404)} \tag{12}$$

The open loop gain ($G(s)H(s)$) of the plant is shown in Fig. 8. The block diagram for experimental verification of self-sensing is shown in Fig. 9. A beam is excited by injecting a white noise signal in the actuator. This white noise acts as an external disturbance. The displacement feedback from the eddy current sensor and self-sensing are used to reduce the effect of the external disturbance on the motion of the free end of the beam. The control force obtained using the displacement feedback is then subtracted from the white noise. First, the feedback from the eddy current sensor is used to see the effectiveness of the designed controller on vibration reduction. The frequency responses of the uncontrolled and controlled structure are compared in Fig. 10a. It can be seen that the designed controller is effective in reducing the vibration of the cantilever beam.

After verification of the controller, the signal obtained from self-sensing is used for the feedback control. The noise in the self-sensed signal drives the actuator which in turn forces the structure to follow the noise. Hence, the signal obtained from the eddy current sensor provides better indication of the performance. The uncontrolled and controlled frequency responses of the beam when self-sensing is used as feedback are compared in Fig. 10b. The feedback from self-sensing is found to exhibit the similar performance as that obtained by using feedback from eddy current sensor for frequencies above 0.2 Hz. The comparison of the controlled and uncontrolled displacement time histories of the beam obtained using self-sensing is shown in Fig. 11. This demonstrates that self-sensing can be effectively used for sensing and actuation simultaneously. An important advantage of self-sensing is that it results in perfectly collocated control.

5. Envisioned application: Drone camera stabilization

Drone camera is subjected to vibrations from the drone which hampers the quality of the captured images. The current system uses passive rubber mounts. These mounts, although effective in reducing the response near resonance, degrade the response at high frequencies (adding damping to the system). Many active mounts have been developed but they work only in one direction [17,18]. This motivated the development of a six degrees of freedom isolation system for drone camera where high quality images are required. The isolation system is based on the cubic configuration of the Stewart platform. The proposed isolation system is shown in Fig. 12. The unique features of the isolation system are — use of non-contact electromagnetic actuators, no flexible joints (clearance between the coil and magnet is used to allow for rotations), 3D printed lightweight parts and high frequency roll-off as there is no stiffness in the legs. Due to the compact architecture and weight limitations, it is not possible to have an array of sensors which can be collocated with the actuators. This motivates the use of self-sensing. It does not require any modifications in the electromagnetic actuators. The voltage drop across each coil can be measured. The measured voltage drop can then be used to evaluate the motion in each of the legs of the isolator. This is then used as a feedback to actively damp the resonances of the isolation system without amplifying the high frequency response. The properties of the system like stiffness may change with time due to fatigue or other environmental factors. Self-sensing provides a robust control strategy which can be useful in such situations. Currently, work is underway to develop a prototype of such isolation system using self-sensing for collocated control.

6. Concluding remarks

In many applications perfect collocation is not possible due to space and size limitations. In such cases, one may resort to self-sensing where a single transducer serves the dual purpose of sensing and actuation. This brief presented self-sensing using electromagnetic actuator. The actuator is operated in current mode. The voltage drop across the coil can be directly measured to evaluate the motion of the coil. No additional bridge structures are required. The measurements from self-sensing have been validated with those obtained using eddy current sensor. The measurements from self-

sensing have also been used to actively control the vibrations of the flexible cantilever beam. The performance of the active control using self-sensing are found to be at par with the active control using an eddy current sensor. Self-sensing provides a robust, cost-effective and simple control architecture. It results in a perfectly collocated system with the guaranteed stability as the open loop transfer function has alternating poles and zeros. It is envisioned to be used for the applications where a large array of sensors could not be used due to space and size limitations.

Authors' contribution

Mohit Verma: conceptualization, methodology, experiments, data curation, investigation, software, writing – original draft. Vicente Lafarga: experiments, data curation, investigation, validation, writing – review & editing. Christophe Collette: conceptualization, funding acquisition, supervision, writing – review & editing.

Declaration of Competing Interest

The authors report no declarations of interest.

Acknowledgements

The authors gratefully acknowledge the Wallonie Region for funding this research (WALInnov Projet Trusteye, Grant No. 1710040). The authors would like to thank Michel Osée for his inputs on current amplifier. The technical discussions with Dimitri Piron and Ahmad Paknejad are also acknowledged.

Appendix A. Circuit diagram of current amplifier

In order to use the electromagnetic actuator in the self-sensing mode, current amplifier is manufactured in-house. The circuit diagram of the current amplifier is shown in Fig. A.13.

Appendix B. Supplementary data

Supplementary data associated with this article can be found, in the online version, at https://doi.org/10.1016/j.sna.2020.112210.

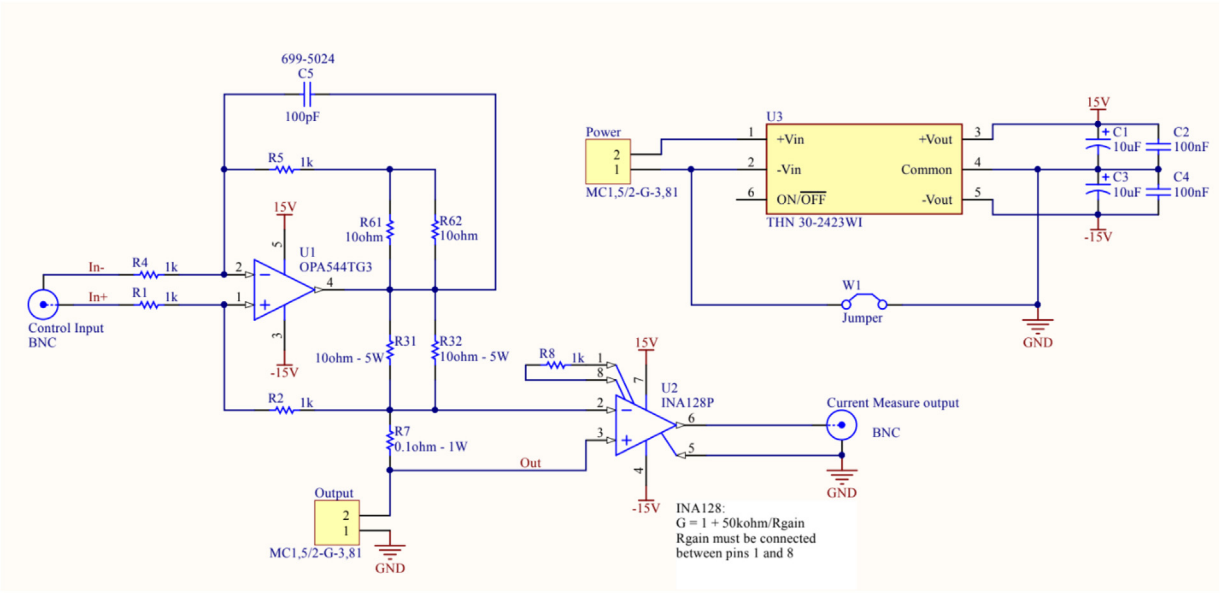

Fig. A.13. Circuit diagram of the current amplified used in the present study.

References

[1] M. Verma, A. Pece, S. Hellegouarch, J. Watchi, G. Durand, S. Chesné, C. Collette, Dynamic stabilization of thin aperture light collector space telescope using active rods, J. Astron. Telesc. Instrum. Syst. 6 (1) (2020) 014002.

[2] C. Collette, F. Matichard, Sensor fusion methods for high performance active vibration isolation systems, J. Sound Vibr. 342 (2015) 1–21.

[3] R. Lorenz, Self-Sensing Motion Control for Electrical and Hybrid Electrical Vehicles, IEE Power Conversions & Applications Lecture, Midlands Engineering Centre, Birmingham, 2001.

[4] X. Xi, D. Chung, Piezoelectret-based and piezoresistivity-based stress self-sensing in steel beams under flexure, Sens. Actuators A: Phys. 301 (2020) 111780.

[5] S.Z. Mansour, R. Seethaler, Simultaneous quasi-static displacement and force self-sensing of piezoelectric actuators by detecting impedance, Sens. Actuators A: Phys. 274 (2018) 272–277.

[6] V. Babuska, R. O'donnell, Self-sensing actuators for precision structures, IEEE, in: 1998 IEEE Aerospace Conference Proceedings (Cat. No. 98TH8339), 1, 1998, pp. 179–187.

[7] J.J. Dosch, D.J. Inman, E. Garcia, A self-sensing piezoelectric actuator for collocated control, J. Intell. Mater. Syst. Struct. 3 (1) (1992) 166–185.

[8] K. Jung, K.J. Kim, H.R. Choi, A self-sensing dielectric elastomer actuator, Sens. Actuators A: Phys. 143 (2) (2008) 343–351.

[9] R. Zhang, P. Iravani, P. Keogh, Closed loop control of force operation in a novel self-sensing dielectric elastomer actuator, Sens. Actuators A: Phys. 264 (2017) 123–132.

[10] S.-H. Lee, S.-W. Kim, Improved position control of shape memory alloy actuator using the self-sensing model, Sens. Actuators A: Phys. 297 (2019) 111529.

[11] G. Hu, Y. Lu, S. Sun, W. Li, Development of a self-sensing magnetorheological damper with magnets in-line coil mechanism, Sens. Actuators A: Phys. 255 (2017) 71–78.

[12] B. Hanson, M. Levesley, Self-sensing applications for electromagnetic actuators, Sens. Actuators A: Phys. 116 (2) (2004) 345–351.

[13] E.O. Ranft, G. Van Schoor, C.P. Du Rand, Self-sensing for electromagnetic actuators. Part II. Position estimation, Sens. Actuators A: Phys. 172 (2) (2011) 410–419.

[14] Y. Okada, K. Matsuda, H. Hashitani, Self-sensing active vibration control using the moving-coil-type actuator, J. Vibr. Acoust. 117 (4) (1995) 411–415, http://dx.doi.org/10.1115/1.2874472.

[15] A. Preumont, Vibration Control of Active Structures: An Introduction, vol. 246, Springer, 2018.

[16] MATLAB, Version 7.8.0.347 (R2009a), The MathWorks Inc., Natick, Massachusetts, 2009.

[17] M. Verma, C. Collette, Active vibration isolation system for drone cameras, in: International Conference on Vibration Problems, 2019, Crete, Greece, ICVOP, 2019, p. Paper ID 18795.

[18] M. Verma, V. Lafarga, M. Baron, C. Collette, Active stabilization of unmanned aerial vehicle imaging platform, J. Vibr. Control (2020), 1077546320905494.

Biographies

Mohit Verma received his Ph.D. in Structural Engineering from AcSIR, India. After that he joined Precision Mechatronics Laboratory at ULB, Belgium as Postdoctoral Research Associate. Currently, he is working as Senior Scientist at CSIR-Structural Engineering Research Centre, India. His area of interest is vibration control of structures.

Vicente Lafarga is a doctoral candidate at the Precision Mechatronics Laboratory at ULB since 2017. His research area focuses on development of a active isolation system for space applications.

Christophe Collette received a M.Sc. and Ph.D. degrees in Mechanical Engineering from the Université Libre de Bruxelles in 2003 and 2007. Christophe Collette is Professor of Mechatronics in the Faculty of Engineering at the Université Libre de Bruxelles and University of Liége. He is the Director of the Precision Mechatronics Laboratory. His main research interests include the active and passive control of vibration, optical inertial sensors and future space telescopes.